ORBITAL CHANGES DURING HYPERSONIC AEROCRUISE[1]

Kenneth D. Mease[2]
Jet Propulsion Laboratory, California Institute of Technology, Pasadena, California

and

Jaemyong Lee[3] and Nguyen X. Vinh[4]
University of Michigan, Ann Arbor, Michigan

Abstract

The orbital changes that occur during an aerocruise maneuver are analyzed using a new mathematical approach. The approach allows the analysis to be conducted in two distinct stages. In the first, the aerodynamic turn is determined, using a nondimensional form of the equations of motion that is free of singularities. We show how the design parameters: speed, altitude, angle of attack, and thrust direction, affect the aerodynamic turn and, in particular, how they should be chosen in order to maximize the aerodynamic turn for a given propellant expenditure. An analytic solution for the aerocruise maneuver is obtained, under certain simplifying assumptions, and is found to be very accurate. The second stage of the analysis concerns the translation of the aerodynamic turn into changes in the orbital elements with respect to the equatorial plane. The translation involves a straightforward transformation of coordinates. The transformation depends on the starting point for aerocruise, i.e., the initial argument of latitude in the initial orbital plane. Analytic solutions for the initial arguments of latitude that maximize the change in inclination and the change in the longitude of the ascending node are given. In the case of maximizing the change in inclination, the analytic solution confirms that the aerodynamic turn should be centered at the nodal crossing. In the case of maximizing the longitude of the ascending node, the analytic solution shows that the best location for the aerodynamic turn depends on the inclination of the initial orbit. Previous claims that the aerodynamic turn should be performed at an apex of the initial orbit have been found to be valid only for an initial inclination of 90°. As the initial inclination decreases towards zero, the optimal location moves from apex towards the node. We also outline a procedure for determining the aerocruise maneuver to achieve a specified orbital plane as defined by particular values of the inclination and the longitude of the ascending node.

Nomenclature

A_R, A_S, A_W	perturbing accelerations: radial, tangential, and binormal
C_L, C_D	lift and drag coefficients
E	aeropropulsive efficiency
I_{sp}	specific fuel consumption
L, D, T	magnitudes of lift, drag, and thrust forces
$\mathbf{R}, \mathbf{V}$	position and velocity vectors
R, V	magnitudes of position and velocity vectors
S	reference surface area
V_C	circular speed
Z	dimensionless altitude
a, e, i, Ω	classical orbital elements
c	dimensionless specific fuel consumption
g	gravitational acceleration
h	angular momentum
k	dimensionless speed
m	vehicle mass
p	semi-latus rectum
$r, \theta, \phi, V, \gamma, \psi$	spherical trajectory variables (Fig. 2)
u	argument of latitude
α, σ	angle of attack; angle of bank
η	thrust direction
μ	dimensionless mass
$\bar{\mu}$	gravitational parameter
ρ	density of atmosphere

Introduction

The reason for considering the use of aerodynamic force, to alter the orbital plane of a spacecraft, is that it often requires less fuel to change the altitude of an orbit (in order to get into the atmosphere and back out) than to rotate the orbit, as noted in the pioneering works of London [1,2] and Nyland [3]. The three basic phases of a synergetic maneuver (i.e., a maneuver effected by a combination of aerodynamic and propulsive forces) are deorbit, atmospheric, and reorbit. In the deorbit phase, propulsive force transfers the vehicle onto an elliptical orbit, that intersects the sensible atmosphere. Likewise, in the reorbit phase, propulsive force transfers the vehicle from the exit orbit, on which it leaves the atmosphere, to the final orbit. In general, changes to the vehicle's orbit, during the atmospheric phase, can be effected by a combination of aerodynamic and propulsive forces. In the so-called *aeroglide* mode, there is no thrusting within the atmosphere. Although substantial propellant savings, over the pure-propulsive plane change, can be realized by the aeroglide mode of synergetic plane change [4], the aeroglide mode has a decidely negative feature. The most efficient gliding aerodynamic turn involves flight at the angle of attack that produces the maximum lift-to-drag ratio, at an angle of bank near 90°, at high speed, and at low altitude where the atmospheric density is high. Unfortunately, this flight program also leads to very high heating rates and consequent thermal protection problems. In order to reduce the heating rate, a high angle of attack entry, which produces high lift and high drag, can be used to reduce speed and cause pull-out at a higher altitude. Furthermore, during the aerodynamic turn, some of the lift force can be used to maintain a high altitude flight path. However, both of these measures compromise the plane change capability.

Another mode of atmospheric flight, known as *aerocruise*, provides an alternative means of achieving an aerodynamic plane change, without incurring high heating rates. Heating rate is a function of density, or altitude, and speed.

[1] The research described in this paper was carried out by the Jet Propulsion Laboratory, California Institute of Technology, under contract with the National Aeronautics and Space Administration.

[2] Member Technical Staff, Navigation Systems Section, Member AIAA

[3] Graduate Student, Aerospace Engineering Department

[4] Professor, Aerospace Engineering Department

A constraint on the maximum heating rate restricts a vehicle's flying condition to a certain region of the altitude-speed space. From the above discussion, the most efficient aerodynamic turn would be achieved in the forbidden region of the altitude-speed space. Thus, it seems reasonable that the most efficient turn, given the heating constraint, would be on the constraint boundary, where the heating rate is equal to its maximum allowable value. Numerical results support this conclusion [5]. The simplest case of flight on the heating rate constraint boundary is flight at a single point on that boundary, i.e., at constant altitude and constant speed. This is generally the flight program that is referred to as aerocruise in the literature. In contrast to aeroglide, aerocruise requires thrusting within the atmosphere. For a given angle of attack, the thrust component along the velocity vector is adjusted to cancel drag. The vertical components of the lift and thrust balance the vehicle's weight minus its centrifugal force, by proper adjustment of the angle of bank. The lateral components of the lift and thrust change the orbital plane. Note that aerocruise, if restricted to constant altitude, constant speed flight, is not a complete atmospheric flight mode. It is the central portion and is preceeded by the descent from the atmospheric entry point, to cruising altitude, and followed by the ascent to the atmospheric exit point.

Under a realistic heating rate constraint, the superiority of aerocruise over both the aeroglide and the pure-propulsive modes for changing the plane of a low orbit (148 km -555 km altitude) has been demonstrated by Cuadra and Arthur [6], Clauss and Yeatmann [7], and Paine [8] in the mid 1960's. Renewed interest in synergetic plane changes has led, more recently, to further study of the aerocruise mode [12,13]. These recent studies have stressed the fact that an orbital plane is defined by not only its inclination (with respect to the equatorial plane), i, but also by the longitude of the ascending node, Ω; and that an aerodynamic turn must be properly located in order to achieve the desired plane change. In [12] and [13], expressions for di/dt and $d\Omega/dt$ are given; and it is shown that di/dt is maximized at either equatorial (nodal) crossing and that $d\Omega/dt$ is maximized at the apexes of the orbit. The implication is that these maxima determine where to conduct the aerodynamic turn to achieve the desired plane change. Approximate analytical results [13] and numerical results [12,13], the latter obtained with the Program to Optimize Simulated Trajectories (POST) [14], support the notion that the greatest inclination change is achieved by centering the aerodynamic turn at the equator. Furthermore, flying at a high angle of attack, in order to maximize the lift coefficient, produces a quicker turn and thus allows more of the turn to occur near the equator, increasing the inclination change. A quicker turn has the added advantage of a reduced total heat load.

In the present paper, a new mathematical approach is used to analyze the aerocruise maneuver. A judicious use of coordinate frames conveniently allows the analysis of the aerocruise maneuver to be conducted in two stages. In the first stage, the focus is on the aerodynamic turn. By using dimensionless variables, the number of parameters, on which aerocruise depends, is reduced to a minimum. A comprehensive study of the influence of cruising speed, cruising altitude, and cruising angle of attack on the magnitude of the aerodynamic turn for a given amount of propellant is presented. The advantages of thrust vectoring are also determined. In the second stage of the analysis, the positioning of the aerodynamic turn to achieve a desired plane change is addressed. It is shown that the aerocruise starting point that maximizes the inclination change or that maximizes the change in the longitude of the ascending node can be determined analytically. The results verify previous claims [12,13] that the aerodynamic turn should be centered at the nodal crossing to maximize the inclination change. However, we find that centering the aerodynamic turn at an apex does not always give the maximum change in the longitude of the ascending node. In addition, a straightforward procedure for solving the problem of how to achieve specified changes in both inclination and nodal angle, using aerocruise, is given. This problem has not been addressed previously. In the first stage of the analysis, the results are obtained numerically, although in a number of special cases approximate analytic solutions are derived and compared to the numerical solutions. In the final section of the paper, an analytic solution for the aerocruise maneuver is derived, and is found to be extremely accurate for inclination changes of up to 40°.

The analysis presented in this paper is restricted to the aerocruise portion of the atmospheric phase. We do not treat the complete maneuver from the initial to the final orbit. On the other hand, most of the aerodynamic plane change would occur during this portion of the atmospheric phase, since the rest of the atmospheric flight would be at lower density and much of the aerodynamic force would have to be directed into the vertical plane to control the altitude changes. Thus, it is reasonable to assume that changes to the plane are effected either during aerocruise or outside the atmosphere. In this case, the analysis presented herein provides the changes in the orbital elements that can be effected during the atmospheric flight.

Plane Change by Aerocruise

A direct approach [13], for determining the orbital changes that occur during aerocruise, is to use the elements of the orbit. We shall follow this approach in this section for the purpose of introducing three problems that arise in connection with the aerocruise maneuver. For a free time problem, we consider the five elements a, e, i, Ω, and u. The flight is conducted at constant altitude and constant speed. The velocity vector $\mathbf{V}$ is perpendicular to the position vector $\mathbf{R}$. The cruising point is then at an apsis of the osculating orbit. By the energy integral

$$V^2 = \bar{\mu}\left(\frac{2}{R} - \frac{1}{a}\right) \tag{1}$$

the semi-major axis is constant. The magnitude of the angular momentum

$$h = RV = \sqrt{\bar{\mu}p} = \sqrt{\bar{\mu}a(1-e^2)} \tag{2}$$

is also constant. Thus the eccentricity is constant. There remain the elements i, Ω, and u which are subject to the three perturbing accelerations, A_R in the radial direction, A_S in the tangential direction, and A_W in the binormal direction. The variations in the elements are given by the classical equations

$$\frac{di}{dt} = \frac{\cos u}{V} A_W \tag{3}$$

$$\frac{d\Omega}{dt} = \frac{\sin u}{V \sin i} A_W \tag{4}$$

$$\frac{du}{dt} = \frac{V}{R} - \frac{\sin u}{V \tan i} A_W \tag{5}$$

For constant altitude, constant speed flight, we have the relations, involving the magnitudes of the lift, drag, and thrust forces,

$$A_S = \frac{T\cos\alpha - D}{m} = 0 \tag{6}$$

$$A_W = \frac{(L + T\sin\alpha)\sin\sigma}{m} \tag{7}$$

$$A_R = \frac{(L + T\sin\alpha)\cos\sigma}{m} = g - \frac{V^2}{R} \tag{8}$$

To these equations, we add the equation for the mass flow

$$\frac{dm}{dt} = -\frac{T}{gI_{sp}} \tag{9}$$

With the usual assumption

$$\begin{aligned} L &= \frac{1}{2}\rho S V^2 C_L(\alpha) \\ D &= \frac{1}{2}\rho S V^2 C_D(\alpha) \end{aligned} \tag{10}$$

and using equation (6) to evaluate T, we write equation (9)

$$\frac{dm}{dt} = -\frac{\rho S V^2 C_D(\alpha)}{2gI_{sp}\cos\alpha} \tag{11}$$

For constant altitude, speed, and angle of attack, the mass flow rate is constant, and m is a linear function of the time. On the other hand, we write equation (8), with the aid of equations (6) and (10)

$$\frac{\cos\sigma}{m} = \frac{2(gR - V^2)\cos\alpha}{\rho S V^2 R C_D[\sin\alpha + (C_L/C_D)\cos\alpha]} \tag{12}$$

The right-hand side is constant and $\cos\sigma$ is proportional to the mass. The bank angle increases as the mass decreases. I.e., as the vehicle's weight minus centrifugal force decreases, the vertical component of lift required to balance the weight decreases. The perturbing acceleration A_W is given explicitly by

$$\begin{aligned} A_W &= \frac{\rho S V^2 C_D[\sin\alpha + (C_L/C_D)\cos\alpha]}{2m\cos\alpha}\sin\sigma \\ &= \frac{(gR - V^2)}{R}\tan\sigma \end{aligned} \tag{13}$$

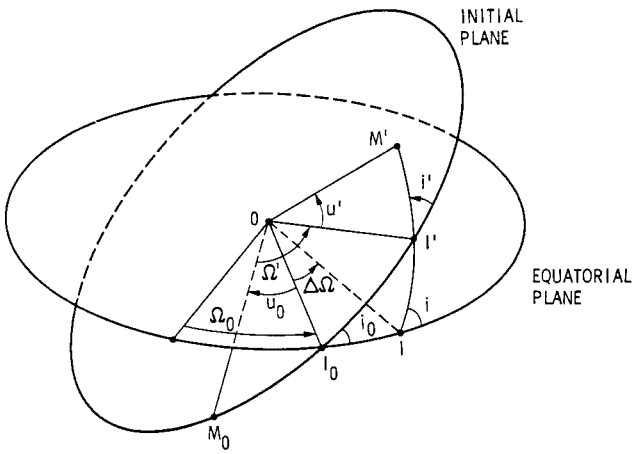

Figure 1. Planes and Angles Involved in Aerocruise Analysis

Cos σ is a well-defined function of the mass, but σ can be either positive or negative (left or right bank). Thus A_W can arbitrarily be chosen as either positive or negative, thereby specifying the direction of the aerodynamic turn.

The autonomous equations (3)-(5) and (9) are integrated, from any given set of initial values i_0, Ω_0, u_0, and m_0, to provide the variations of the elements i, Ω, and u, as functions of either m or t. Fig. 1 shows the position of the initial plane, as defined by the inclination i_0 and the longitude of the line of the ascending node Ω_0. Let M_0 be the starting point for the cruise. It is defined by the initial argument of the latitude u_0. In the following, we assume that i_0 and m_0 are given and, without any loss of generality, that $\Omega_0 = 0$. The parameter u_0 acts as a control parameter, in that, its value, i.e., the location of the starting point for aerocruise, determines whether the ensuing aerodynamic turn provides a change in the inclination, a change in the longitude of the ascending node, or a combination of the two. As an indication of this, equations (3) and (4), show that, when $\cos u \approx 0$, i is near stationary; while, when $\sin u \approx 0$, Ω is near stationary. (We shall show later, however, that for finite duration maneuvers, it is not always best to locate aerocruise where suggested by these stationary conditions.) Several aerocruise problems and corresponding solution procedures are as follows.

1. Orbital Plane Change. It is proposed to achieve, for a specified initial mass m_0, the final orbital plane as defined by the given values i_f and Ω_f. For this problem, we integrate from a guessed value u_0 to the final condition i_f. The final value of Ω obtained is compared with the given value Ω_f for concordance. The solution is obtained by iteration on u_0. This also gives the final mass m_f. Note that physically, there will be a constraint on how small m_f can become. There may be pairs (i_f, Ω_f) that can not be achieved with the available propellant mass $m_0 - (m_f)_{min}$.

2. Maximum Change in the Inclination. The inclination change $\Delta i = |i_0 - i_f|$ depends on u_0 for a fixed m_f. We search for the value u_0 that maximizes Δi, obtained by integrating to m_f.

3. Maximum Change in the Longitude of the Node. Similarly, the node change $\Delta\Omega = |\Omega_0 - \Omega_f|$ depends on u_0 for a fixed m_f. We search for the value u_0 that maximizes $\Delta\Omega$, obtained by integrating to m_f.

While the problem (1.) is not discussed in [12,13], problems (2.) and (3.) were addressed. In [12] and [13], the solutions to problems (2.) and (3.) were initially inferred from equations (3) and (4). Since the rates of change of inclination and node angle, are maximized at the nodes and at the apexes, respectively, it was suggested that the aerodynamic turn should be centered at a node to maximize Δi or at an apex to maximize $\Delta\Omega$. In [12], the solution procedure described above for problem (2.) was carried out using POST. The numerical results, for the particular input data used, support the hypothesis that the maximum Δi is achieved by centering the aerodynamic turn at the node. Furthermore, high angle of attack flight produces the largest Δi by allowing a quicker turn, thereby concentrating the turn in the region of maximum sensitivity (i.e., near the node). In [13], analytic solutions for equations (3)-(5) were derived under certain simplifying assumptions. The approximate solutions were compared to numerical solutions generated by POST. The solution for Δi was found to be quite accurate. The accuracy of the solution for $\Delta\Omega$ is dependent on the value of the inclination of the initial orbit. The solution is quite accurate for an initial inclination of 90°, but it grows worse as the

initial inclination decreases. For a particular case, the analytical and numerical results confirm that Δi is maximized by centering the aerodynamic turn at the node. The hypothesis regarding the maximization of $\Delta\Omega$ by centering the turn at an apex is not tested in either [12] or [13].

In the following sections, the aerocruise maneuver is analyzed using a new mathematical approach. The equations describing the vehicle motion during aerocruise are reformulated using a nondimensional form of the trajectory variables. The equations are free of singularities. (Note that equations (3)-(5) have singularities at zero inclination.) In the nondimensional formulation, the number of influencing physical parameters is reduced to a minimum; the effects of altitude, speed, angle of attack, and thrust direction can be displayed explicitly for a general class of aerospace vehicles. It will be shown that the three basic problems mentioned above can be solved explicitly without iteration on the parameter u_0. This is done by computing the trajectory using the initial plane as the reference plane and deducing the trajectory, relative to any other reference plane, by a simple coordinate transformation.

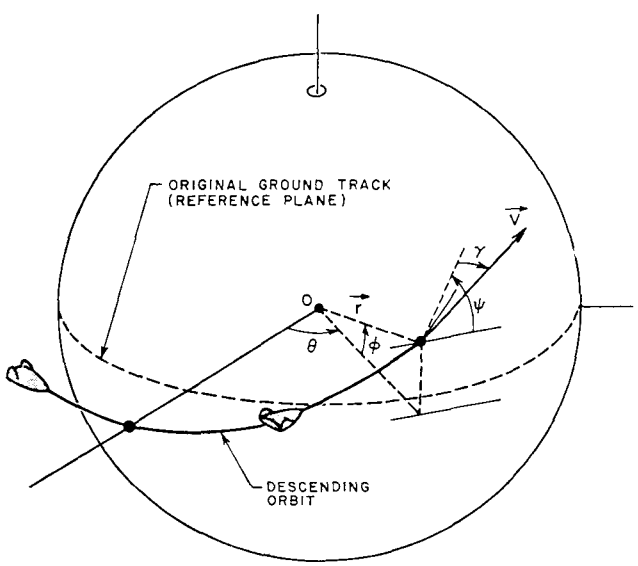

Figure 2. Coordinate System

Dimensionless Equations of Aerocruise

In this new approach, we use the spherical trajectory variables $(r, \theta, \phi, V, \gamma, \psi)$ with the initial plane taken as the reference plane (Fig. 2). We have the equations of motion [15]

$$\frac{dr}{dt} = V \sin\gamma \tag{14}$$

$$\frac{d\theta}{dt} = \frac{V \cos\gamma \cos\psi}{r \cos\phi} \tag{15}$$

$$\frac{d\phi}{dt} = \frac{V \cos\gamma \sin\psi}{r} \tag{16}$$

$$\frac{dV}{dt} = A_S - g \sin\gamma \tag{17}$$

$$V\frac{d\gamma}{dt} = A_R - g\cos\gamma + \frac{V^2}{r}\cos\gamma \tag{18}$$

$$V\frac{d\psi}{dt} = \frac{A_W}{\cos\gamma} - \frac{V^2}{r}\cos\gamma\cos\psi\tan\phi \tag{19}$$

For constant altitude flight, $\gamma = 0$ and $r = R$; and, if the cruise is at constant speed, we immediately have

$$A_S = 0, \qquad A_R = \frac{gR - V^2}{R} \tag{20}$$

These are precisely the conditions (6) and (8) obtained above.

With the equations for r, V, and γ satisfied by the steady solution, we consider the three remaining equations in θ, ϕ, and ψ. In steady spherical flight, the time is proportional to the dimensionless arc length s such that

$$\frac{ds}{dt} = \frac{V}{R} \tag{21}$$

Using s as the new independent variable, we have the equations

$$\frac{d\theta}{ds} = \frac{\cos\psi}{\cos\phi} \tag{22}$$

$$\frac{d\phi}{ds} = \sin\psi \tag{23}$$

$$\frac{d\psi}{ds} = \frac{Z}{\mu}\sin\sigma - \cos\psi\tan\phi \tag{24}$$

where we have defined the dimensionless mass

$$\mu = \frac{m}{m_0} \tag{25}$$

and the constant parameter

$$Z = \left(\frac{\rho S R}{2m_0}\right)\left(\frac{C_D}{\cos\alpha}\right)\left[\sin\alpha + \left(\frac{C_L}{C_D}\right)\cos\alpha\right] \tag{26}$$

Equation (11) for the variation of the mass can be put in the dimensionless form

$$\frac{d\mu}{ds} = -\frac{1}{ck}\frac{Z}{E} = -\mu' \tag{27}$$

where μ' is the mass flow rate and E is the aeropropulsive efficiency

$$E = \sin\alpha + \left(\frac{C_L}{C_D}\right)\cos\alpha \tag{28}$$

and the constant k and c are defined as

$$k = \frac{\sqrt{gR}}{V} = \frac{V_C}{V}, \qquad c = I_{sp}\sqrt{\frac{g}{R}} \tag{29}$$

In terms of these same parameters and variables, the bank control law as given in equation (12) has the new form

$$\frac{\cos\sigma}{\mu} = \frac{(k^2 - 1)}{Z} \tag{30}$$

By inspection of the equations, the advantages of the new formulation are clear. Instead of the three equations (3), (4) and (5) in the orbital elements i, Ω, and u, we now have the three equations (22), (23) and (24) in the variables θ, ϕ, and ψ. The new equations are free of singularities. In

addition, the need for iteration in the arbitrary parameter u_0 has been eliminated. We simply integrate forward the three equations with the initial conditions well defined as

$$s = 0, \qquad \mu_0 = 1, \qquad \theta_0 = \phi_0 = \psi_0 = 0 \tag{31}$$

The trajectory generated can then be related to the trajectory for any specified set of values (i_0, u_0) by a coordinate transformation as discussed in the next section.

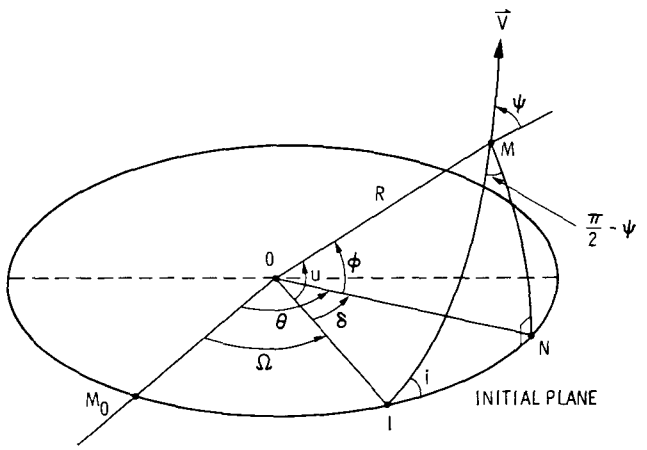

Figure 3. Geometry of Trajectory Variables and Orbital Elements with Respect to the Initial Plane

Fig. 3 shows the geometry of the variables (θ, ϕ, ψ) and the orbital elements (i, Ω, u) with the initial plane as reference plane. Let M_0 be the starting position of the vehicle in the initial plane and M be the position of the vehicle at time t in the osculating plane OIM. From the right spherical triangle INM, we have the relations

$$\cos i = \cos\phi \cos\psi \tag{32}$$

$$\cos u = \cot i \tan\psi \tag{33}$$

$$\tan u = \frac{\tan\phi}{\sin\psi} \tag{34}$$

$$\sin\phi = \sin u \sin i \tag{35}$$

These redundant relations relate the two sets of variables (ϕ, ψ) and (i, u). As for the change in the longitude of the ascending node, we have

$$\Omega = \theta - \delta \tag{36}$$

where the angle δ is obtained from any one of the following relations

$$\begin{aligned} \sin\delta &= \tan\phi \cot i \\ \sin\phi &= \tan\delta \tan\psi \\ \sin\psi &= \cos\delta \sin i \\ \cos u &= \cos\delta \cos\phi \end{aligned} \tag{37}$$

In the new formulation, through the use of dimensionless parameters and variables, the number of influencing physical parameters has been reduced to a minimum. To analyze the performance, we first specify the dimensionless specific fuel consumption c, as defined in equation (29). This is a characteristic of the propulsion system. Next, to perform the integration, we need to specify the mass ratio $\mu_f = \frac{m_f}{m_0}$ and three physical parameters, Z, k, and E. The parameter k is the ratio of the circular speed to the cruising speed. By the control law (30), it is seen that when $k > 1$, the cruising speed is subcircular and the bank angle is less than 90°. The lift is directed upward and the cruising point is at the apogee of the osculating orbit. On the other hand, when $k < 1$, the cruising speed is supercircular, and the lift is directed downward with the bank angle greater than 90°. The cruising point is at the perigee of the osculating orbit. The parameter Z is essentially the altitude parameter, since it is proportional to the density ρ. For constant angle of attack, by varying Z, we vary the cruising altitude. We notice that the actual weight of the vehicle, and its size, are contained in Z. Hence, the analysis is valid for a whole class of vehicles having similar aerodynamic characteristics.

Aerocruise Performance Factors

To study the effect of the altitude, cruising speed, and angle of attack (via E) on inclination change performance, we first compute a baseline trajectory using the values

$$\begin{aligned} Z &= 0.286326 \\ \mu' &= 0.399511 \\ k &= 1.083836 \\ \mu_f &= 13/21 \end{aligned} \tag{38}$$

These values correspond essentially to the data used in [13]. The integration, from the initial mass $\mu_0 = 1$, to the final mass μ_f, provides the final values for the trajectory variables

$$\theta = 0.944598, \qquad \phi = 0.118670, \qquad \psi = 0.263412 \tag{39}$$

which correspond to the changes in the elements of the orbit

$$i = 16.520761°, \quad u = 24.603748°, \quad \Omega = 30.419491° \tag{40}$$

From this baseline trajectory, we consider first the effect of the altitude by varying the value of Z, while keeping the same speed ratio k and the same angle of attack (or, equivalently, the same value of E). From the definition of μ', reproduced here for convenience,

$$\mu' = \frac{1}{ck}\frac{Z}{E} \tag{41}$$

we take, consistent with [13], the value $c = 0.353612$, which corresponds to $I_{sp} = 290$ seconds, and an angle of attack such that $E = 1.87$. Then, for each value of Z, we compute the corresponding value of μ' and compute the change in inclination for the same mass ratio $\mu_f = 13/21$. The results are shown in Fig. 4.

We notice that the effect of the altitude is very general since we do not have to specify the physical dimensions and mass of the vehicle. On the abscissa, we have the change in linear altitude in dimensionless form. If we consider an exponential atmosphere

$$\rho = \rho_0 e^{-\beta z} \tag{42}$$

then using the baseline altitude, we have the linear change

$$\beta z = \ln\left(\frac{\rho_0}{\rho}\right) = \ln\left(\frac{Z_0}{Z}\right) \tag{43}$$

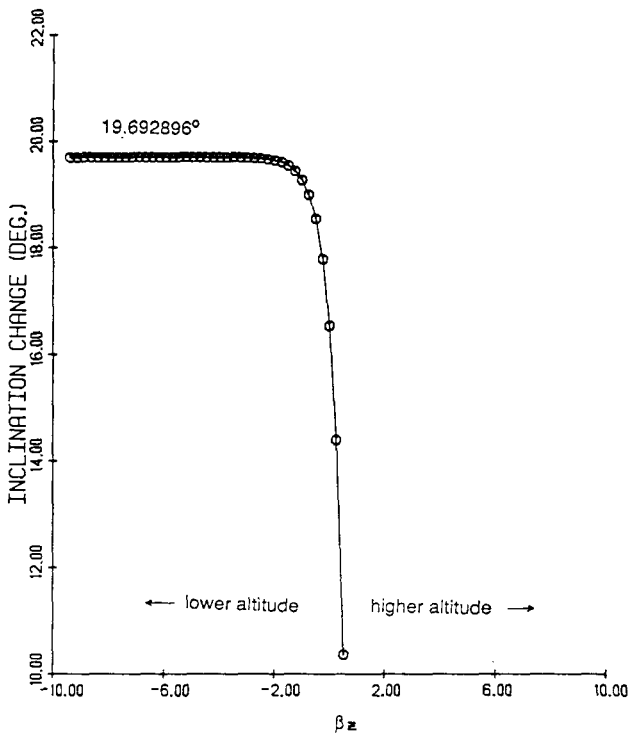

Figure 4. Effect of the Altitude on Plane Change

Fig. 4 shows that the inclination change increases as the altitude decreases. Hence, for fixed mass ratio, cruising speed, and angle of attack, the optimum altitude is the lowest altitude. The cruising time is also shorter. However, getting to a lower altitude, while maintaining a high cruising speed, may require thrusting before the initiation of aerocruise. Also, exiting from low altitude will require additional thrusting. Any additional thrusting will reduce the amount of fuel, $m_0 - (m_f)_{min}$, available for aerocruise. This is not taken into account in the generating the results shown in Fig. 4, since the available fuel is assumed to be the same at each altitude. Furthermore, severe heating will be encountered at low altitude. Thus, it is still preferable to cruise at a relatively high altitude. From Fig. 4, the maximum plane change tends asymptotically to the value $i = 19.692896°$. Mathematically, this is obtained by making Z very large. From the bank control law (30), the limiting bank angle is 90°. Then, for large value of Z, equation (24) becomes

$$\frac{d\psi}{ds} = \frac{Z}{\mu} \tag{44}$$

Using equation (27) to change the independent variable to the mass, we obtain the equation

$$\frac{d\psi}{d\mu} = -\frac{ckE}{\mu} \tag{45}$$

which can be integrated to give

$$\psi = ckE\ln(1/\mu_f) \tag{46}$$

At high lift, the turn is nearly instantaneous, that is $\phi \approx 0$, and this heading change is also the inclination change, which is readily computed to be $i = 19.692896°$.

We next consider the effect of the cruising speed on the inclination change. This is obtained by varying k, while keeping the altitude and the angle of attack at their baseline values. From the definition (26), we keep Z constant at the value $Z = 0.286326$. Then, for various values of k, we compute μ' from equation (41), with the same values for c and E as given above. From the numerical integration, we have the plot in Fig. 5. It is seen that there exists an optimal value of the cruising speed slightly less than the circular speed. From equation (30), we see that all of the aerodynamic force can be used for turning ($\sigma = \pm 90°$), if $k = 1$, i.e., if the cruising speed is circular speed. On the other hand, the duration of the aerodynamic turn, which also helps determine the amount of inclination change, decreases as the speed increases. This occurs because the mass flow rate is proportional to the speed, as shown in equation (27). The best compromise, for the particular altitude and angle of attack under consideration, is to fly at slightly less than circular speed. However, we shall see later (Fig. 11), that the optimal cruising speed is not always so close to circular speed.

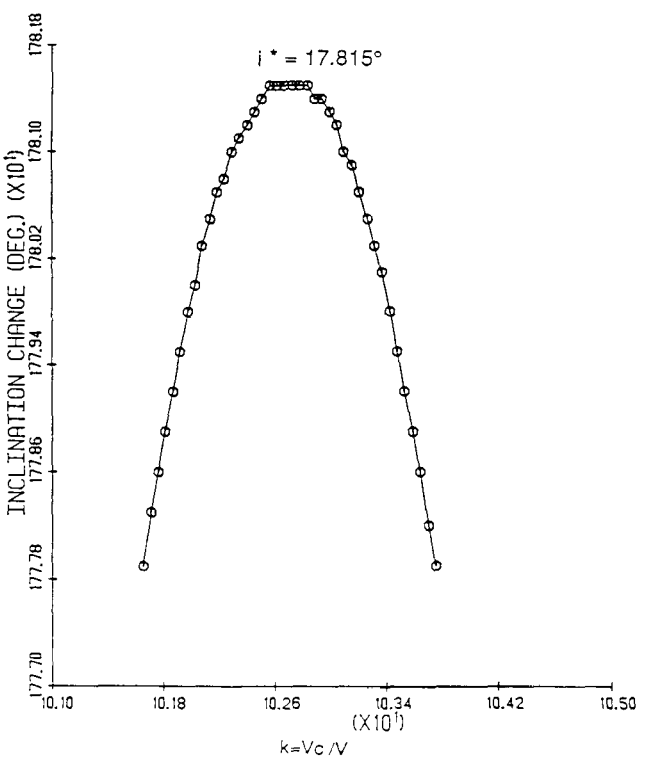

Figure 5. Effect of Speed on Plane Change

Finally, we consider the effect of the angle of attack on the inclination change. This requires the modeling of the aerodynamic characteristics. We shall assume the aerodynamic characteristics given in [16]. Fig. 6 shows the variations of the lift and the drag coefficients, C_L and C_D as function of α; while Fig. 7 shows the variation of the lift-to-drag ratio, C_L/C_D, and the aeropropulsive efficiency E. By polynomial curve fitting, we have the following functions with α expressed in radians

$$
\begin{aligned}
C_L &= -2.068686996\alpha^3 + 2.943200144\alpha^2 \\
&\quad + 0.080347684\alpha + 0.031320026 \\
C_D &= 0.267339707\alpha^3 + 1.814473159\alpha^2 \\
&\quad - 0.389985867\alpha + 0.068372034
\end{aligned} \tag{47}
$$

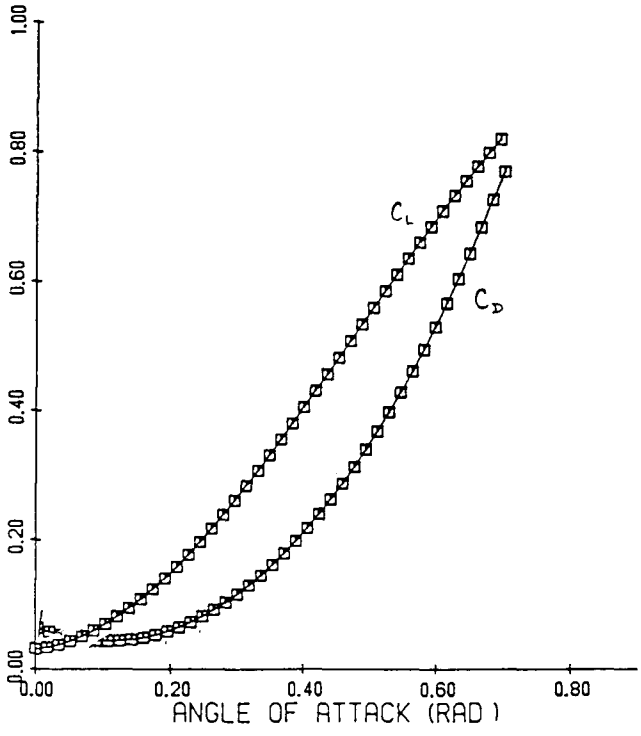

Figure 6. The Variation of the Lift and Drag Coefficients as Functions of the Angle of Attack

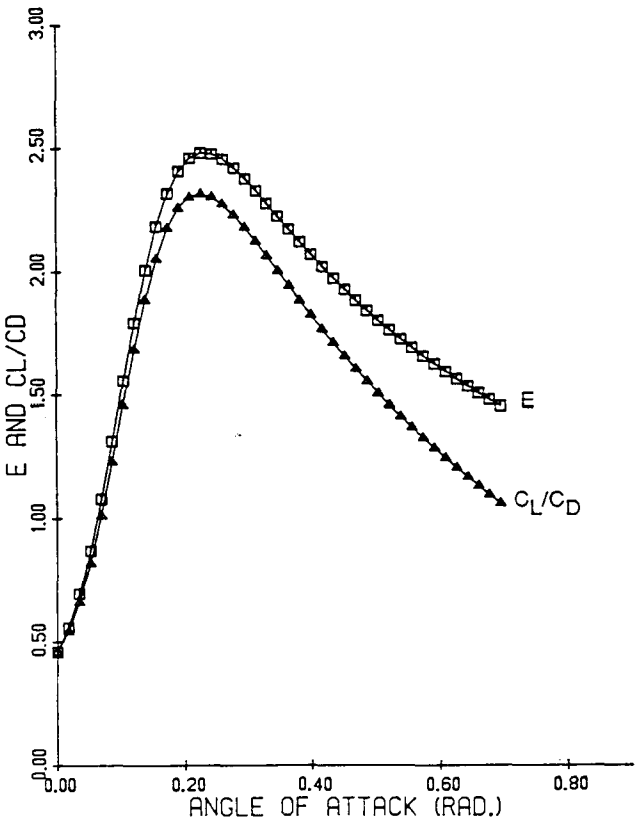

Figure 7. The Variation of the Lift-to-Drag Ratio and the Aeropropulsive Efficiency as Functions of the Angle of Attack

The value $E = 1.87$ used for the baseline trajectory corresponds to the high angle of attack $\alpha = 27.32°$. With this, we compute the value $C_D/\cos\alpha = 0.364710$, and hence, for the baseline altitude, we have the value $\bar{Z} = \rho SR/(2m_0) = 0.419828$ or

$$
Z = 0.419828(C_D/\cos\alpha)E \tag{48}
$$

For each α, we evaluate Z and compute μ' from equation (41). The speed ratio k and the mass ratio μ_f are kept at their baseline values. From the numerical integration, we have the variation of i as a function of α as shown in Fig. 8(a). It is seen that the maximum of i occurs at the value $\alpha = 28.6°$, which is near the value $\alpha = 27.32°$ used for the baseline trajectory. The corresponding maximum inclination is $i = 16.58°$.

The greater effectiveness of aerocruise at high lift coefficient (i.e., high angle of attack), rather than at maximum lift-to-drag ratio, has been noted previously [12]. In fact, for the baseline altitude, as represented by Z, aerocruise at maximum lift-to-drag ratio is not possible. To see this, examine the control law (30). As the mass μ decreases, the bank angle σ increases. At the start of aerocruise, we must have the minimum condition, $|\cos\sigma| \leq 1$, at the initial time when $\mu = 1$; that is

$$
Z \geq |k^2 - 1| \tag{49}
$$

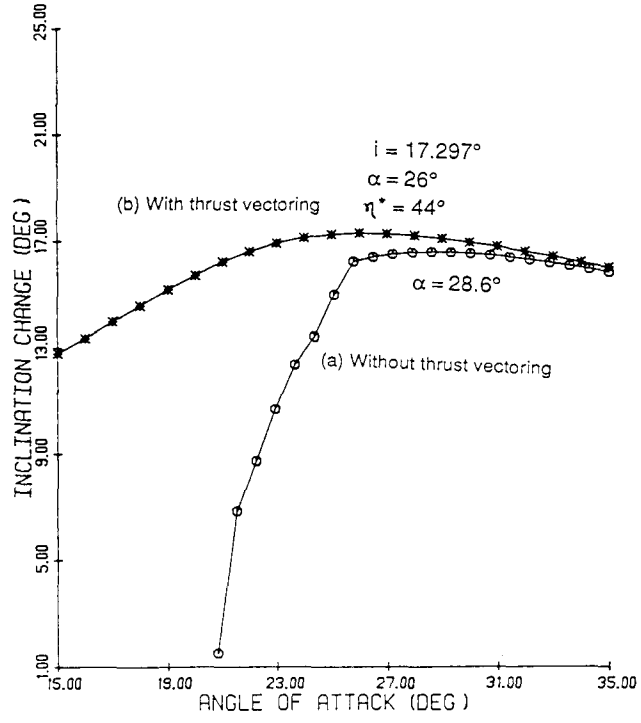

Figure 8. The Variation of Plane Change as a Function of the Angle of Attack

If the density Z is less than this value, the lift generated is not sufficient to maintain constant altitude flight, even without turning. From equation (48), with the selected value of k, this corresponds to $\alpha \geq 20.77°$. Since the maximum lift-to-drag ratio is achieved at $\alpha = 13°$, aerocruise at maximum lift-to-drag ratio is not possible.

The analysis thus far has assumed that the thrust line is fixed in the vehicle and this line is along the body axis from which the angle of attack is measured. We now use the same body axis to measure the angle of attack, but with the new assumption that the engine can be rotated, in the plane defined by the lift and drag vectors, to change the thrust direction. Let η be the angle between the thrust vector and the velocity vector. The modification in the equations consists of changing the definition of Z to

$$Z = \left(\frac{\rho S R}{2m_0}\right)\left(\frac{C_D}{\cos\eta}\right)[\sin\eta + (C_L/C_D)\cos\eta] \qquad (50)$$

and of the aeropropulsive efficiency to

$$E = \sin\eta + (C_L/C_D)\cos\eta \qquad (51)$$

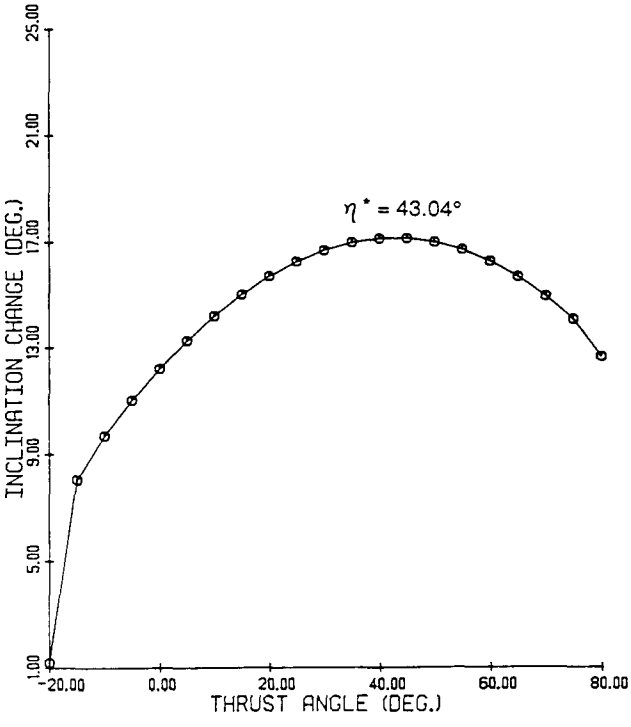

Figure 9. The Effect of the Thrust Angle on Plane Change ($\alpha^* = 28.6°$)

The same values for c, k, and $(\rho S R/2m_0)$ are used and the two angles α and η are now treated as control parameters. Fig. 9 shows the results for the optimum angle of attack $\alpha^* = 28.6°$ with different values of the thrust angle η. It is seen that there exists an optimal value $\eta^* = 43.04°$ providing a higher inclination $i = 17.15°$. The same process is repeated for other values of the angle of attack and the net performance is plotted as curve (b) in Fig. 8. The over all best performance is $i = 17.297°$ obtained with $\alpha = 26°$ and $\eta = 44°$. Another advantage of thrust vectoring, as is clearly seen in the Fig. 8, is that now the aerocruise can be performed at low angle of attack for vehicle with an insufficiently high lift coefficient. For example, if we restrict the angle of attack to be such that $\alpha \leq \alpha_{max} = 20°$, aerocruise is not possible at constant altitude with the selected speed, even without turning. But, if thrust vectoring is permitted to add a component $T\sin\eta$ in the direction of the lift, then aerocruise is feasible.

It has been shown by Bell and Hankey [9] and Nyland [10] that, if the bank angle is assumed to be constant during aerocruise, the optimum thrust angle is such that

$$\tan\eta = \frac{1}{L/D} \qquad (52)$$

where

$$L/D = C_L/C_D \qquad (53)$$

is the lift-to-drag ratio used for aerocruise. As compared to the true optimum thrust angle with the bank angle varying, as it should, according to the control law (30), formula (52) gives a much lower value. Also, the trend for optimum thrust vectoring is not correct. It is possible to obtain a more accurate formula for the optimum thrust angle. In this respect, when the variation in the latitude is small, we can neglect the centrifugal acceleration in equation (24) to have

$$\frac{d\psi}{ds} = \frac{Z}{\mu}\sin\sigma \qquad (54)$$

Then, using equation (27) to change the independent variable from s to μ, we obtain

$$\frac{d\psi}{d\mu} = -\frac{ckE}{\mu}\sin\sigma \qquad (55)$$

As seen from equation (30), the bank angle monotonically increases as the mass decreases during the cruise. Hence we can use this equation to change the independent variable to σ. This gives

$$d\sigma = -\frac{d\mu}{\mu\tan\sigma} \qquad (56)$$

Equation (55) becomes

$$d\psi = (ckE)\frac{\sin^2\sigma}{\cos\sigma}d\sigma \qquad (57)$$

which can be integrated to give

$$\psi = (ckE)\left\{\ln\left[\frac{\cos\sigma_0(1+\sin\sigma_f)}{\cos\sigma_f(1+\sin\sigma_0)}\right] + \sin\sigma_0 - \sin\sigma_f\right\} \qquad (58)$$

A more rigorous analytical solution will be provided in the last part of the paper. Here, this approximate solution is designed to study the effect of the thrust angle on turning performance. The heading change ψ, as given in equation (58) is a function of η through the aeropropulsive efficiency, E, and the terminal bank angles, σ_0 and σ_f, such that

$$\cos\sigma_0 = \frac{(k^2-1)}{Z}, \qquad \cos\sigma_f = \frac{(k^2-1)\mu_f}{Z} \qquad (59)$$

with Z being a function of η as shown in equation (50). By maximizing the function ψ, we also maximize the latitude ϕ as shown in the state equation (23); the higher values of ψ and ϕ will render higher values of the inclination change i as given in equation (32). By writing the condition for a stationary value of ψ with respect to η, we have the optimum condition

$$\cos\eta[\cos\eta - (L/D)\sin\eta]\left\{\ln\left[\frac{\cos\sigma_0(1+\sin\sigma_f)}{\cos\sigma_f(1+\sin\sigma_0)}\right] + \sin\sigma_0 - \sin\sigma_f\right\} + (\sin\sigma_f - \sin\sigma_0) = 0 \tag{60}$$

The optimum value of η as given by this equation is plotted versus α in Fig. 10. It is lower than the optimum value obtained by exact numerical integration, but is substantially more accurate than the value obtained from equation (52). Also the numerical solution of equation (60) shows correctly that η decreases as α increases. We note that Bell and Hankey [9] arrive at equation (52) by rewriting equation (54) as $d\psi/d(\ln\mu) = -ckE\sin\sigma$ and then differentiating with respect to η to find where the magnitude of the derivative is maximized. The value of η given by equation (52) is the value that maximizes the aeropropulsive efficiciency E. However, the bank angle σ is also a function of η. Equation (52) neglects this dependence and does not give the optimum thrust direction as a result.

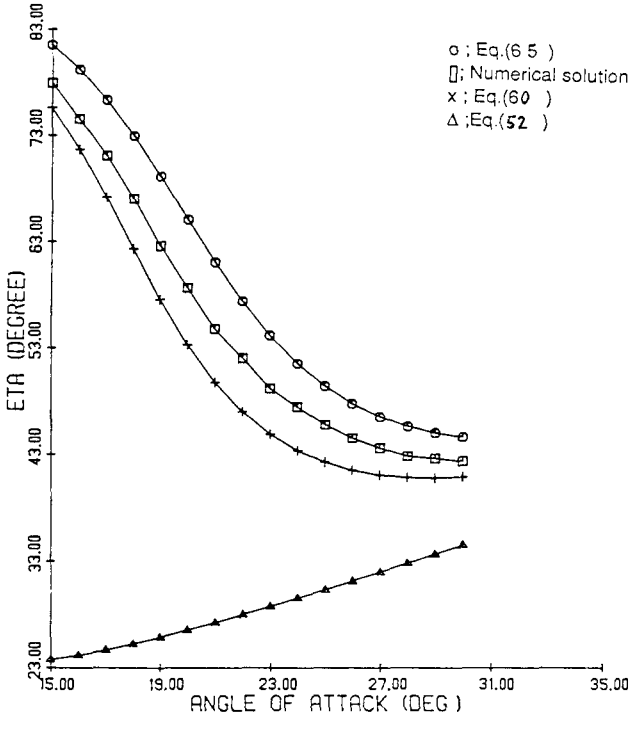

Figure 10. The Optimal Thrust Angle as a Function of the Angle of Attack

A simple solution of the transcendental equation (60) can be found by considering only the first order in the change in the bank angle. Then

$$\cos\sigma_f = \cos(\sigma_0 + \Delta\sigma) = \cos\sigma_0 - (\sin\sigma_0)\Delta\sigma$$
$$\sin\sigma_f = \sin(\sigma_0 + \Delta\sigma) = \sin\sigma_0 + (\cos\sigma_0)\Delta\sigma \tag{61}$$

Upon substituting into equation (60), linearizing the logarithm, and simplifying by the common factor $\Delta\sigma \neq 0$, we have the simple equation

$$\cos\eta[\cos\eta - (L/D)\sin\eta]\sin^2\sigma_0 + \cos^2\sigma_0 = 0 \tag{62}$$

Let

$$A = \frac{2m_0(k^2-1)}{\rho S R C_D} \tag{63}$$

and notice that

$$\cos\sigma_0 = \frac{A}{[\tan\eta + (L/D)]} \tag{64}$$

Upon substituting into equation (62), we have a quadratic equation for $\tan\eta$

$$(L/D)\tan^2\eta + [(L/D)^2 - A^2 - 1]\tan\eta - L/D = 0 \tag{65}$$

Its solution, which is slightly higher than the exact solution, is also plotted in Fig. 10.

The approximate heading angle solution (58) can also be used to analyze the effect, on inclination change, of the cruising altitude and the cruising speed, as has been done numerically before. First, ψ is a function of altitude, as represented by the dimensionless density Z. By taking the derivative of this equation with respect to Z, we have

$$\frac{d\psi}{dZ} = \frac{(ckE)}{Z}(\sin\sigma_f - \sin\sigma_0) > 0 \tag{66}$$

Hence the heading change, and correspondingly the inclination change, increases as the density increases. When Z becomes very large, equation (58) tends to equation (46), the approximation developed earlier. Second, the heading angle ψ is a function of the speed, as represented by the speed ratio k. By writing the condition for a stationary value of ψ with respect to k, we have, after some algebraic manipulation, the condition

$$(k^2-1)\left[\ln\frac{(1+\sin\sigma_f)}{\mu_f(1+\sin\sigma_0)}\right] + (3k^2-1)(\sin\sigma_0 - \sin\sigma_f) = 0 \tag{67}$$

where of course σ_0 and σ_f are functions of k as given in equation (59).

As before, an approximate solution of equation (67) can be obtained by using the linearized trigometric functions (61). Again, in order to cancel the factor $\Delta\sigma$, we write the logarithm in equation (67)

$$\ln\frac{(1+\sin\sigma_f)}{\mu_f(1+\sin\sigma_0)} = \ln\frac{\cos\sigma_0}{(1+\sin\sigma_0)}\frac{(1+\sin\sigma_f)}{\cos\sigma_f} \approx \frac{\Delta\sigma}{\cos\sigma_0}$$

Then equation (67) in its simplified form becomes

$$(k^2-1) - (3k^2-1)\cos^2\sigma_0 = 0$$

Using equation (59), we have a biquadratic equation

$$3k^4 - 4k^2 + (1 - Z^2) = 0 \tag{68}$$

with the solution

$$k^2 = \frac{1}{3}(2 + \sqrt{1 + 3Z^2}) \tag{69}$$

We have repeated the numerical experiment in Fig. 5 for several altitudes starting from the baseline altitude and for each altitude searched for the optimum value of k. We have also used equation (67) and its approximate solution (69) for calculation of the optimum value of k. We find that equation (67), resulting from the optimization of the approximate equation (58), provides excellent results as shown in Fig. 11. In fact, to the resolution of Fig. 11, they are identical. The solution given in equation (69) is also plotted in Fig. 11, and besides its simplicity, the result is fairly accurate, in that it shows the correct trend of the optimum speed. This speed decreases as the altitude decreases.

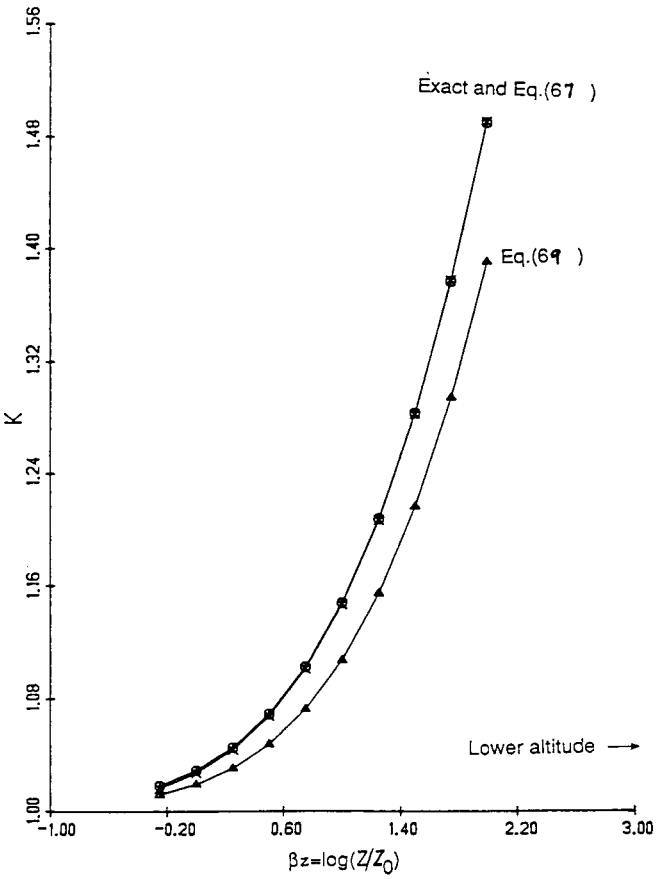

Figure 11. The Optimum Speed Ratio as a Function of the Altitude

It was suggested in the Introduction that aerocruise is best performed on the heating rate constraint boundary in altitude-speed space. With this in mind, it is of interest to determine where along this constraint boundary the maximum inclination change can be achieved. Assuming that the heating rate is proportional to $\rho^{.5}V^3$, the value of this quantity was computed for the baseline case. Then the altitude and speed were varied so as to maintain the same heating rate. For each variation, the inclination change was computed. For example, if aerocruise was performed at a lower altitude (higher density), then the speed would have to be reduced, in order not to exceed the baseline heating rate. Fig. 12 shows the result. The altitude is the dominating factor. As found earlier, the achievable inclination change increases as the altitude decreases. However, it is interesting to see the effect of the speed, which is not held at the baseline value, as was the case in Fig. 4, but varies with altitude according to the heating constraint. As illustrated in Fig. 11, there is a speed that maximizes the inclination change, for a given altitude. Along the heating constraint boundary, the speed is closest to optimal at an altitude of approximately 70.5 km. This gives rise to a local maximum in the curve shown in Fig. 12. Without considering the fuel required to deorbit to and reorbit from a low altitude aerocruise, it is impossible to draw any conclusion as to the optimal aerocruise altitude. However, the presence of the local maximum is attractive from a guidance point of view, since there is a range of altitudes over which the inclination change is relatively constant.

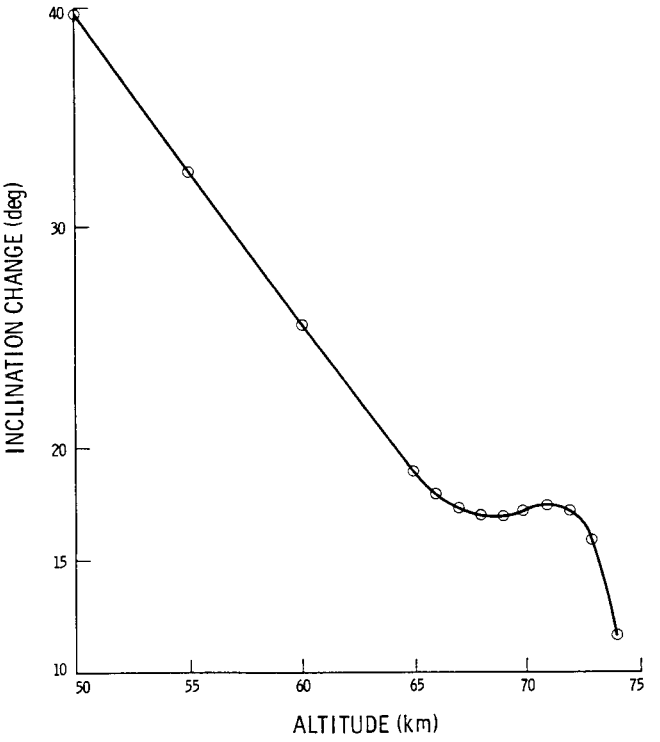

Figure 12. Inclination Change Along Heating Constraint Boundary

In summary, the present formulation leads to a differential system free of singularities, which can be integrated with the minimum number of entry data required. This allows us to analyze the effects on performance of the altitude, speed, angle of attack, and thrust direction for a general class of vehicles, since the size and the actual mass of the vehicle do not have to be specified. The only physical data involved are the specific fuel consumption I_{sp}, which characterizes the propulsion system used, and the aerodynamic characteristics of the vehicle in terms of the functions $C_L(\alpha)$ and $C_D(\alpha)$. Other influencing factors used are dimensionless and of a general nature. More specifically, for the fuel consumption, we just need to specify the mass ratio $\mu_f = m_f/m_0$. The cruising speed is expressed as the ratio, $k = V_C/V$, of the circular speed to the cruising speed. It is sufficient to introduce any realistic value of

$$\bar{Z} = \frac{\rho S R}{2m_0} \tag{70}$$

as a baseline value. Then we can interpret a change in Z, say a reduction in Z, as higher altitude flight (smaller ρ), or as a higher mass-to-surface area ratio (higher m_0/S) vehicle at the same altitude.

Coordinate Transformation

We have generated a baseline aerocruise trajectory and analyzed the effect of altitude, speed, angle of attack, and thrust direction on inclination change by using the initial plane as the reference plane. In practice, the equatorial plane is the reference plane and the initial plane has the inclination i_0 as shown in Fig. 1. We shall use the prime notation to denote the variables computed using the initial plane as the reference plane, that is to say the primed variables are the variables computed in the previous section. The variables with respect to the equatorial plane can be easily deduced by a simple coordinate transformation on the sphere with radius R.

In Fig. 1, M_0 is the initial point and M' is the point at the time t. The integration in the previous section provides the elements i', Ω', u', ... The actual new inclination is i, with the change being $\Delta i = i - i_0$. The actual change in the longitude of the ascending node is the angle $I_0OI = \Delta\Omega$ (and not Ω' as computed previously). Along the initial orbit, the point M_0, which is the point where we initiate aerocruise, is defined by the angle $u_0 = \angle I_0OM_0$, called the initial argument of latitude. This angle is measured in the initial plane, from the initial line of the ascending node OI_0. In Fig. 1, u_0 is negative. From the oblique spherical triangle I_0II' with the sides and angles as labeled, we have

$$\cos i = \cos i_0 \cos i' - \sin i_0 \sin i' \cos(\Omega' + u_0) \quad (71)$$

$$\cos i' = \cos i_0 \cos i + \sin i_0 \sin i \cos \Delta\Omega \quad (72)$$

$$\frac{\sin \Delta\Omega}{\sin i'} = \frac{\sin(\Omega' + u_0)}{\sin i} \quad (73)$$

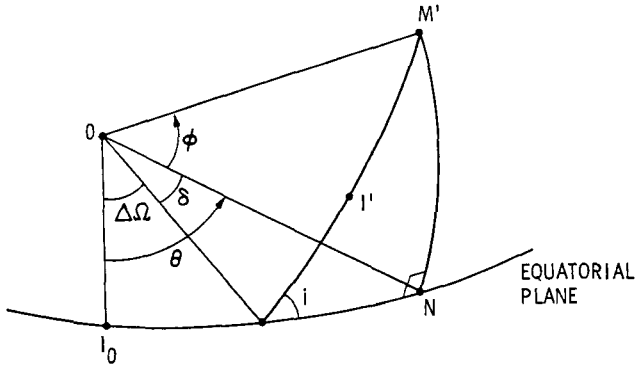

Figure 13. Longitude and Latitude with Respect to the Equatorial Plane

The last equation is redundant, but it may be useful in some calculations. We can now solve the following problems.

a. Computation of the Actual Variables. With a single integration, we have generated and stored the primed variables i' and Ω' as functions of the time. Now, for any prescribed i_0 (initial inclination with respect to the equatorial plane) and u_0 (initial cruising point selected in the initial orbit), we can use equation (71) to compute the actual inclination i, and hence the inclination change $\Delta i = i - i_0$. Next, the actual change of the nodal angle $\Delta\Omega$ is given by equation (72). To compute the longitude θ of the vehicle, as measured in the equatorial plane from the initial line of the ascending node OI_0, and its latitude ϕ, we consider the right spherical triangle $IM'N$ (Fig. 13). First we compute the arc $\widehat{IM'} = u = \widehat{II'} + \widehat{I'M'} = \widehat{II'} + u'$ (refer to Fig. 1). The angle u' has been computed through the integration of the baseline trajectory. As for the arc $\widehat{II'}$, from the oblique spherical triangle I_0II', it is most easily obtained by the law of sines

$$\frac{\widehat{II'}}{\sin i_0} = \frac{\Delta\Omega}{\sin i'} \quad (74)$$

Once the angle u has been computed, we simply have

$$\sin\phi = \sin u \sin i \quad (75)$$

$$\cos\delta = \frac{\cos u}{\cos\phi} \quad (76)$$

$$\theta = \Delta\Omega + \delta \quad (77)$$

b. Changing the Orbital Plane. In aeroassisted orbital transfer, aerocruise is used to effect a change to a new orbital plane as specified by the inclination i and the longitude of the ascending node $\Delta\Omega$. This fundamental problem is not solved in [12] or [13]. A search for both the unknown parameter u_0 specifying the initial cruising point M_0 and the time of flight would be required to achieve both the prescribed conditions on i and $\Delta\Omega$. In the present formulation, besides removing the singularity in the equations of motion, the problem can be solved in a straightforward manner, without an iterative search for the unknown parameters. First, for any prescribed final inclination $i = i_f$, and longitude of the ascending node $\Delta\Omega = \Delta\Omega_f$, we obtain the angle i' from equation (72). Then using the equations in the previous section (in θ', ϕ', and ψ'), we integrate until we obtain $\cos i' = \cos\phi' \cos\psi'$. As products of the integration, we obtain the required final mass μ_f, the time of flight, and Ω'. Finally, equation (71) can be solved for u_0, giving the position M_0 where aerocruise should be initiated.

c. Maximizing the Inclination. For a prescribed initial inclination i_0 and fuel consumption, in terms of the mass ratio μ_f, the initial point M_0, i.e., the value of u_0, influences the net inclination change Δi, since, if the cruise is conducted near the line of nodes, the rate of change in the inclination is maximized. This problem has been addressed in [12,13]. In the present formulation, the solution is obtained in closed form. For this purpose, we simply rewrite equation (71) as

$$\cos i = \cos(i_0 + i') + 2 \sin i_0 \sin i' \sin^2 \frac{1}{2}(\Omega' + u_0) \quad (78)$$

From this relation, it is clear that

$$i \le i_0 + i' \quad \text{or} \quad \Delta i \le i'$$

The actual plane change Δi is always less or at most equal to the plane change i' computed, with

a specified μ_f, using the initial plane as the reference plane. The maximum Δi is obtained when $\sin \frac{1}{2}(\Omega' + u_0) = 0$, that is for the value

$$u_0 = -\Omega' \tag{79}$$

The point M_0, as defined explicitly by this solution, must be before the point I_0, which indicates the initial line of the ascending node. (Note that $u_0 = -\Omega' + 180°$ is also a solution.) Using this solution in equation (73), it is seen that

$$\Delta\Omega = 0 \tag{80}$$

In the flight program that maximizes the change in the inclination, the net change in the line of nodes is zero. In Fig. 1, the triangle $I_0 I I'$ is reduced to a point. In a heuristic fashion, we may say that the aerocruise arc is distributed evenly around the node; although, this is not rigorously true, since the osculating plane is varying during the flight.

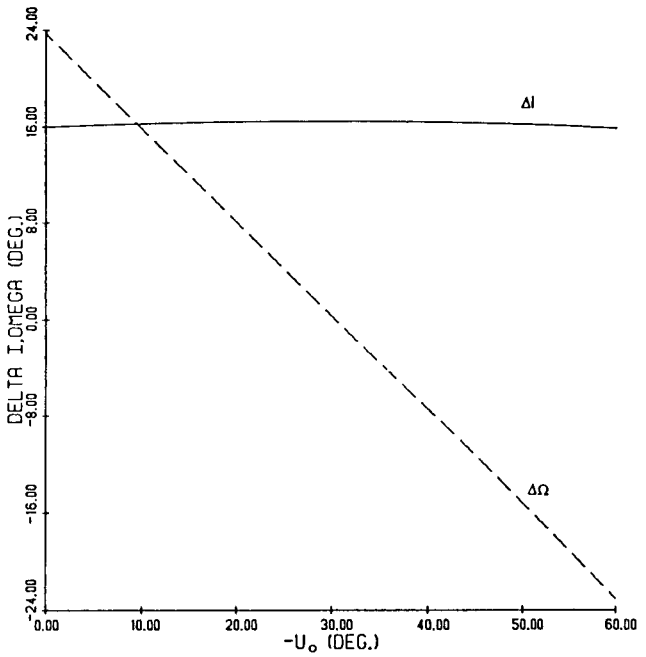

Figure 14. Effect of Initial Argument of Latitude on Change in Inclination

We have used the baseline trajectory, as given in equation (40), with $i' = 16.52°$ and $\Omega' = 30.42°$, and plotted, in Fig. 14, the inclination change, $\Delta i = i - i_0$, and the corresponding nodal angle change $\Delta\Omega$, as functions of the initial argument of latitude u_0, according to equations (71) and (72). The initial angle is taken to be $i_0 = 5°$, in order to display the fact that the present formulation is not handicapped by the smallness of the initial inclination. Although the maximum Δi is difficult to locate in Fig. 14, it does occur at $u_0 = -30.42°$, consistent with equation (79). At $u_0 = -30.42°$, $\Delta\Omega = 0$ as predicted. The insensitivity of Δi to u_0 is a result of the small initial inclination we have chosen. In fact, if we take $i_0 = 0$, then $i = i'$; any starting point M_0 will lead to the same inclination change due to the rotational symmetry. As the value of i_0 increases, the sensitivity of Δi to u_0 increases.

d. Maximizing the Change in the Line of Nodes. This problem has also been addressed in [13], through the use of POST, but it appears that some inaccuracies in the results occur when large changes in Ω are involved. Here, we obtain an explicit solution to the problem and use it to explain the singularity that occurs when the equatorial plane is taken as the reference plane.

We have seen in the preceeding section that, for a prescribed μ_f, the angles i' and Ω' are uniquely determined by forward integration. For a given i_0, by equation (72), $\Delta\Omega$ is a function of i, which is in turn a function of u_0 by equation (71). By taking the derivative of equation (72) with respect to i and setting $d\Delta\Omega/di = 0$, we obtain

$$\cos \Delta\Omega = \frac{\tan i}{\tan i_0} \tag{81}$$

Substituting back into equation (72), we have the relation

$$\cos i_0 = \cos i \cos i' \tag{82}$$

Using this solution in equation (71), we obtain

$$-\cos(\Omega' + u_0) = \frac{\tan i'}{\tan i_0} \tag{83}$$

Since i' and Ω' are known from the baseline solution, we can obtain from equation (83), for each given i_0, the solution u_0 which maximizes the change in Ω. The inclination is given by equation (82); the maximum change in the longitude of the ascending node is given by equation (81). For the solution to exist, it is clear from equation (82) that we must have

$$i' \leq i_0 \tag{84}$$

To see the effect of the initial inclination i_0 for the cases of maximum Δi and maximum $\Delta\Omega$, we refer to Figs. 15 and 16. In Fig. 15, we plot the maximum Δi and maximum $\Delta\Omega$ versus i_0. The maximum $\Delta i = i' = 16.52°$, independent of the initial inclination. In fact, it is always true that the maximum Δi is independent of the initial inclination. As for the maximum $\Delta\Omega$, it is given by equation (81), with the value i computed from equation (82). The maximum $\Delta\Omega$ decreases as i_0 increases. When the initial inclination i_0 is equal to the maximum possible change in inclination i', $i = 0$ and $\cos \Delta\Omega = 0$, i.e., the limiting value of the change in the longitude of the ascending node is $\Delta\Omega = 90°$. It is interesting that, when $i_0 \leq i'$, the vehicle can always maneuver to rotate the initial plane to coincide with the equatorial plane. Then, Ω is undefined and $\Delta\Omega$ can be anywhere from 0° to 360°. When $i_0 = 90°$, $i = 90°$. To obtain the limiting value of $\Delta\Omega$, as i_0 approaches 90°, we rewrite equation (81) as

$$\cos \Delta\Omega = \frac{\sin i}{\cos i} \frac{\cos i_0}{\sin i_0} = \frac{\sin i}{\sin i_0} \cos i' \tag{85}$$

Thus, the maximum $\Delta\Omega$ approaches i' as i_0 approaches 90°. In physical terms, when the initial orbit is a polar orbit, the

maximum $\Delta\Omega$ is the same as the inclination change i' relative to the initial polar orbit. The roles of the inclination and the longitude of the ascending node are simply reversed in going from the polar frame to the equatorial frame. Fig. 15 is the same as Fig. 6 in [13], but there the graph indicates that $\Delta\Omega$ does not approach 90° as i_0 approaches i', as it should. This is probably due to the fact that, in this case, i tends to zero and the singularity caused by $\sin i$ in the denominator, in the equations used in [13], introduces a large error in the integration.

In previous studies [12,13], it has been claimed that $\Delta\Omega$ is maximized by centering the aerodynamic turn at an apex. In our formulation, the angular position of the center of the aerodynamic turn, relative to the node (I_0), is given roughly by $\Omega' + u_0$ (see Fig. 1). For example, equation (79) validates the claim that the maximum Δi is achieved by centering the turn at the node ($\Omega' + u_0 = 0°$). For the case of maximum $\Delta\Omega$, equation (83) shows that the optimal location ($\Omega' + u_0$) is a function of the initial inclination i_0. For an initial polar orbit ($i_0 = 90°$), the optimal location is at apex. However, as i_0 decreases towards i', the optimal location moves from apex to node.

It has also been suggested [12,13] that, when $\Delta\Omega$ is maximized, the corresponding Δi is small. For the case of maximum Δi, we have seen that the corresponding value for the node angle change is $\Delta\Omega = 0$. For the case of maximum $\Delta\Omega$, we have plotted Δi versus i_0 in Fig. 16. For $i_0 = 90°$, $i = 90°$ and $\Delta i = 0$. When $i_0 = i' = 16.52°$, $i = 0$, i.e., the final plane is the equatorial plane for the maximum change in the line of the ascending node. Hence, $|\Delta i| = 16.52°$. Again, a similar plot in [13] exhibits some inaccuracies in this case. It is clear from Fig. 16 that Δi can be anywhere from 0 to i'. It is only for large values of i_0, that Δi is small.

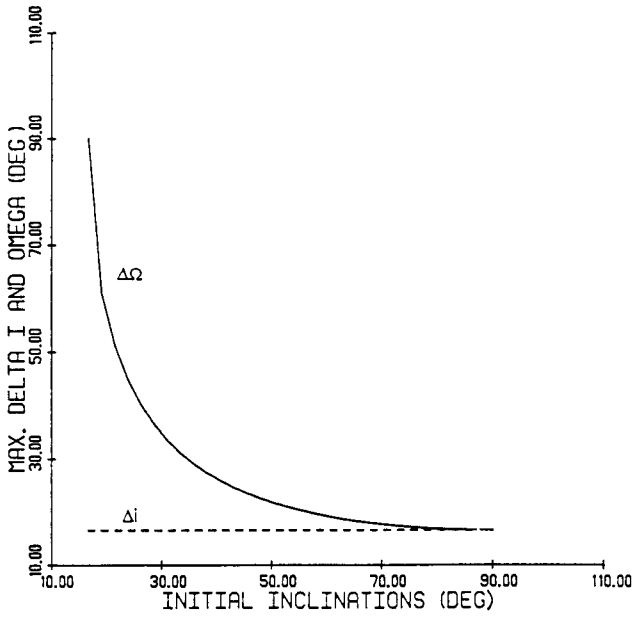

Figure 15. Maximum Δi and Maximum $\Delta\Omega$ versus i_0

Analytic Integration

If the latitude and heading angles are assumed small, i.e., if sines and cosines of these angles are approximated by the first term in their respective Taylor series expansions, a series solution to equations (22)- (24) can be obtained. As with the numerical solution, this analytic solution provides longitude, latitude, and heading angles, which can in turn be converted to inclination and longitude of the ascending node, all relative to the initial trajectory plane. To obtain these angles, relative to any other reference plane, simply requires a nonlinear coordinate transformation, as described in the previous section. The derivation of the analytic solution follows.

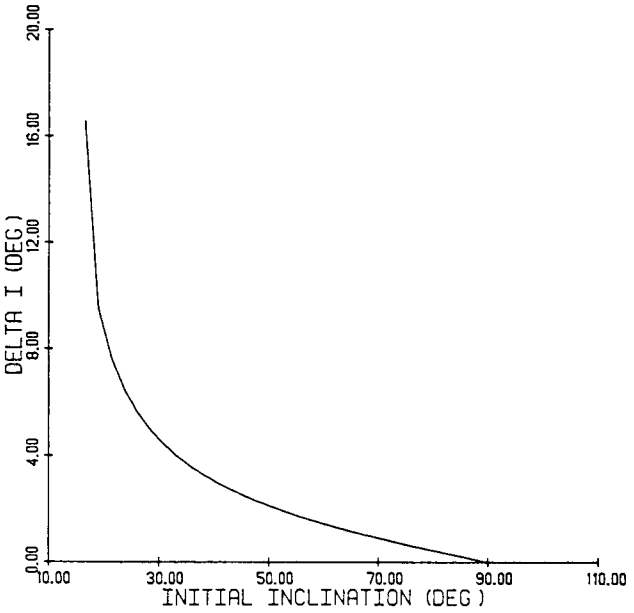

Figure 16. Inclination Change versus Initial Inclination for Maximum $\Delta\Omega$

With the small angle approximation, equations (22)-(24) become

$$\frac{d\theta}{ds} = 1 \tag{86}$$

$$\frac{d\phi}{ds} = \psi \tag{87}$$

$$\frac{d\psi}{ds} = -\phi + \frac{Z}{\mu} - \frac{(k^2-1)^2}{2Z}\mu - \frac{(k^2-1)^4}{8Z^3}\mu^3 - \cdots \tag{88}$$

where $\sin\sigma$ in equation (24) has been replaced by the exact series expansion

$$\sin\sigma = \sqrt{1-\cos^2\sigma} = 1 - \frac{1}{2}\cos^2\sigma - \frac{1}{8}\cos^4\sigma - \cdots$$
$$= 1 - \frac{\mu^2(k^2-1)^2}{2Z^2} - \frac{\mu^4(k^2-1)^4}{8Z^4} - \cdots \tag{89}$$

using the relationship between $\cos\sigma$ and the variables μ, k, and Z provided by the control law (30). In terms of a new independent variable

$$x = \mu/\mu'$$

and the new parameters

$$\epsilon = (k^2-1)^2/2 \qquad \text{and} \qquad b = Z/\mu',$$

equations (86)-(88) become

$$\frac{d\theta}{dx} = -1 \tag{90}$$

$$\frac{d\phi}{dx} = -\psi \tag{91}$$

$$\frac{d\psi}{dx} = \phi - \frac{b}{x} + \epsilon\frac{x}{b} + \epsilon^2\frac{x^3}{2b^3} + \ldots \tag{92}$$

using equation (27).

Integrating from $x_0 = 1/\mu'$ to $x_f = \mu_f/\mu'$, the solution to equation (90) is simply

$$\theta = x_0 - x \tag{93}$$

Combining equations (87) and (88) yields

$$\frac{d^2\psi}{dx^2} + \psi = \frac{b}{x^2} + \frac{\epsilon}{b} + \frac{3\epsilon^2 x^2}{2b^3} + \cdots \tag{94}$$

The homogeneous equation has the solution

$$\psi = A\cos x + B\sin x \tag{95}$$

with A and B constants. According to the variation of parameters approach, the homogeneous solution is assumed to provide the form of the complete solution to equation (94), with A and B considered now as functions of x. It can then be shown that the variables A and B should satisfy the equations

$$\frac{dA}{dx} = -\left(\frac{b}{x^2} + \frac{\epsilon}{b} + \frac{3\epsilon^2}{2b^3}x^2 + \cdots\right)\sin x \tag{96}$$

$$\frac{dB}{dx} = \left(\frac{b}{x^2} + \frac{\epsilon}{b} + \frac{3\epsilon^2}{2b^3}x^2 + \cdots\right)\cos x \tag{97}$$

In integrating these equations, the terms involving powers of ϵx greater than two shall be neglected. These terms, however, present no particular difficulty and could be retained if necessary. The truncated expressions are quite accurate for σ near 90°. If σ takes on values farther from 90°, more terms will be needed.

The solution of the truncated form of equation (94), obtained by integrating the truncated forms of equations (96) and (97) and substituting the results into the solution form provided by the homogeneous solution (95), is

$$\begin{aligned}\psi =& C_1\cos x + C_2\sin x + \frac{\epsilon}{b} + \frac{3\epsilon^2}{2b^3}(x^2-2)\\ &- b\Big[\sin x\Big(x - \frac{x^3}{3\cdot 3!} + \frac{x^5}{5\cdot 5!} - \frac{x^7}{7\cdot 7!} + \frac{x^9}{9\cdot 9!} - \cdots\Big)\\ &+ \cos x\Big(\ln x - \frac{x^2}{2\cdot 2!} + \frac{x^4}{4\cdot 4!} - \frac{x^6}{6\cdot 6!} + \frac{x^8}{8\cdot 8!} - \cdots\Big)\Big]\end{aligned} \tag{98}$$

Since

$$\phi = \frac{d\psi}{dx} + \frac{b}{x} - \frac{\epsilon x}{b} - \frac{\epsilon^2 x^3}{2b^3}$$

it follows that

$$\begin{aligned}\phi =& -C_1\sin x + C_2\cos x + \frac{b}{x} - \frac{\epsilon x}{b}\Big[1 + \frac{\epsilon}{2b^2}(x^2-6)\Big]\\ &- b\Big[\cos x\Big(\frac{1}{x} + \frac{x}{2!} - \frac{x^3}{3\cdot 4!} + \frac{x^5}{5\cdot 6!} - \frac{x^7}{7\cdot 8!} + \frac{x^9}{9\cdot 10!} - \cdots\Big)\\ &+ \sin x\Big(1 - \ln x + \frac{x^2}{2\cdot 3!} - \frac{x^4}{4\cdot 5!} + \frac{x^6}{6\cdot 7!} - \frac{x^8}{8\cdot 9!} + \cdots\Big)\Big]\end{aligned} \tag{99}$$

Using the initial conditions $\psi(x_0) = 0$ and $\phi(x_0) = 0$ to evaluate the constants C_1 and C_2, we obtain

$$\begin{aligned}\psi(x) =& \, b\cos x\ln(x_0/x) + A(x) - A(x_0)\cos(x_0 - x)\\ &+ b[C(x_0) - C(x)]\sin x - b[D(x_0) - D(x)]\cos x\\ &+ [B(x_0) + b\cos x_0 D'(x_0)\\ &- b\sin x_0 C'(x_0)]\sin(x_0 - x)\end{aligned} \tag{100}$$

and

$$\begin{aligned}\phi(x) =& -b\sin x\ln(x_0/x) - A(x_0)\sin(x_0 - x)\\ &+ b[C(x_0) - C(x)]\cos x + b[D(x_0) - D(x)]\sin x\\ &+ [B(x) + b\cos x D'(x) - b\sin x C'(x)]\\ &- [B(x_0) + b\cos x_0 D'(x_0)\\ &- b\sin x_0 C'(x_0)]\cos(x_0 - x)\end{aligned} \tag{101}$$

where

$$\begin{aligned}A(x) &= \frac{\epsilon}{b}\Big[1 + \frac{3\epsilon}{2b^2}(x^2-2)\Big]\\ B(x) &= \frac{b(1-\cos x)}{x} - \frac{\epsilon x}{b}\Big[1 + \frac{\epsilon}{2b^2}(x^2-6)\Big]\\ C(x) &= \sum_{n=1}^{\infty}(-1)^{n+1}\frac{x^{2n-1}}{(2n-1)(2n-1)!}\\ D(x) &= \sum_{n=1}^{\infty}(-1)^{n+1}\frac{x^{2n}}{(2n)(2n)!}\end{aligned} \tag{102}$$

The series $C(x)$ and $D(x)$ and their derivatives with respect to x, $C'(x)$ and $D'(x)$, are all convergent.

We have compared the analytic solutions (93), (100), and (101) with the "exact" solutions to equations (22)-(24), obtained by numerical integration, and found them to be very accurate. Fig. 17 shows that the inclination only begins to exhibit a perceptible error above 40°.

Summary

An analysis of the changes in the orbital plane that can be effected during aerocruise has been conducted in two stages. In the first stage, trajectory variables and orbital elements are defined with respect to the initial orbital plane. In this reference frame, the inclination is initially zero, and the change in inclination is equal to the inclination at the end of the aerocruise maneuver, i'. The starting point for aerocruise, as measured by u_0', has no bearing on the achievable i', in this reference frame, due to the spherical symmetry. (Consideration of Earth rotation, winds, or a nonspherical gravitational potential would, in general, destroy this symmetry.) Thus, u_0' can be taken as zero, with no loss of generality. By numerically integrating equations (22)-(24), subject to the bank control law (30) and the initial conditions (31) or by using the analytic solutions (93), (100), and (101), the values of θ, ϕ, and ψ at the end of the aerocruise maneuver

are computed. Then, using equations (32)- (37), the achieved i', Ω', and u', with respect to the initial orbital plane (refer to Fig. 1), are computed. The achieved i' is the measure of the magnitude of the aerodynamic turn. It sets the limits on the actual (with respect to the equatorial reference frame) plane change that is achieved; specifically, the actual $\Delta i \leq i'$. We have shown how the choices of constant altitude, speed, angle of attack, and thrust direction affect the value of i'. Furthermore, the nondimensional mathematical formulation of the problem is free from singularities and minimizes the number of input data, such that the results apply to a wide range of vehicles and flight regimes.

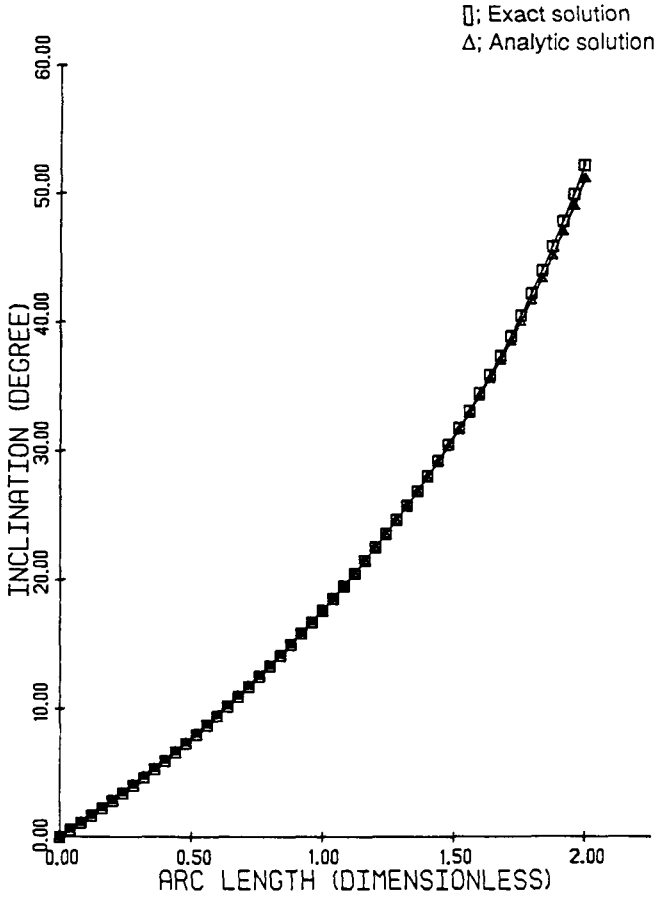

Figure 17. Inclination versus Dimensionless Arc Length

In the second stage of the analysis, the effect of the aerodynamic turn on the orbital elements, defined with respect to the equatorial plane, is studied. The orbital elements, i and Ω, that define the new orbital plane, with respect to the equatorial plane, are computed using the transformations (71) and (72). The transformations are general in the sense that they operate solely on i' and Ω', the integrated effects of the aerodynamic turn; whether i' and Ω' were produced by constant altitude, constant speed flight or otherwise is immaterial. These transformations do depend on the starting point of aerocruise, u_0. The value of u_0 that maximizes Δi is determined by the simple formula (79). Physically speaking, the aerodynamic turn should be centered around either of the nodal crossings to maximize Δi. When Δi is maximized, $\Delta\Omega$ is always zero. The values of u_0 that maximize $\Delta\Omega$ are given by equation (83). When $\Delta\Omega$ is maximized, the corresponding value of Δi depends on the initial inclination, i_0; the value of Δi goes from 0° to i' as i_0 goes from 90° to i'. When $i_0 \leq i'$, the orbit can always be made equatorial and thus $\Delta\Omega$ can be anywhere from 0° to 360°. As i_0 goes from 90° to i', the location of the aerodynamic turn that maximizes $\Delta\Omega$ goes from the apex to the node. This fact was not realized in previous studies. We have also given a method for determining the aerocruise maneuver to achieve specified values of i and Ω.

Conclusion

The orbital changes that occur during an aerocruise maneuver have been analyzed by using a new mathematical approach. The approach allows the analysis to be conducted in two distinct stages. In the first, the aerodynamic turn is determined, using a nondimensional form of the equations of motion that is free of singularities. We have shown how the design parameters: speed, altitude, angle of attack, and thrust direction, affect the aerodynamic turn and, in particular, how they should be chosen in order to maximize the aerodynamic turn for a given propellant expenditure. The second stage of the analysis concerns the translation of the aerodynamic turn into changes in the orbital elements with respect to the equatorial plane. The translation involves a straightforward transformation of coordinates. The transformation depends on the starting point for aerocruise, i.e., the initial argument of latitude in the initial orbital plane. Analytic solutions for the initial arguments of latitude that maximize the change in inclination and the change in the longitude of the ascending node have been given. In the case of maximizing the change in inclination, the analytic solution confirms that the aerodynamic turn should be centered at the nodal crossing. In the case of maximizing the longitude of the ascending node, the analytic solution shows that the best location for the aerodynamic turn depends on the inclination of the initial orbit. Previous claims that the aerodynamic turn should be performed at an apex of the initial orbit have been found to be valid only for an initial inclination of 90°. As the initial inclination decreases towards zero, the optimal location moves from apex towards the node. We have also outlined a procedure for determining the aerocruise maneuver to achieve a specified orbital plane as defined by particular values of the inclination and the longitude of the ascending node.

A fact that has been brought by our analysis and that in [12] is that flight at high angle of attack (i.e., high lift coefficient) produces a larger inclination change than flight at maximum lift-to-drag ratio. This is an apparent contradiction to the conventional wisdom. However, much of the work in the past on synergetic plane changing did not consider vehicle heating. Without a constraint on heating rate, the total characteristic velocity for a synergetic plane change is minimized by diving deep into the atmosphere (50-60 km altitude) and performing the aerodynamic turn under high dynamic pressure. In this case, the turn is completed relatively quickly for either the angle of attack for maximum lift-to-drag ratio or the angle of attack for high lift. I.e., the aerodynamic turn, at high dynamic pressure, takes place over such a short range, in any case, that the fact that the turn at high lift is somewhat quicker is unimportant. On the other hand, turning at maximum lift-to-drag ratio does offer an advantage in energy efficiency and is therefore preferred. Now, when a realistic heating rate constraint is imposed, the aerodynamic turn must be performed at lower dynamic pressure and consequently the turn takes place over a longer range. The fact that the turn can be quicker at high lift becomes important for achieving the desired plane change. Thus the solution has changed because the problem statement has changed.

The analysis in this paper has focused on the aerocruise mode of a synergetic plane change maneuver. The analysis is incomplete in that only the aerocruise portion of the complete maneuver has been addressed. Nevertheless, it is very useful to have a theory for how the orbital plane changes during aerocruise. Most of the aerodynamic plane change would occur during this portion of the maneuver, since the rest of the atmospheric flight would be at lower density and much of the aerodynamic force would have to be directed into the vertical plane to control the altitude changes. The mathematical formulation presented here has made apparent the generic properties of hypersonic aerocruise.

References

1. LONDON, H.S., "Change of Satellite Orbit Plane by Aerodynamic Maneuvering," *Journal of the Aerospace Sciences*, Vol. 29, No. 3, March 1962, pp. 323-332.

2. LONDON, H.S., "Comments on Aerodynamic Plane Change," *AIAA Journal*, Vol. 1, No. 10, October 1963, pp. 2414-2415.

3. NYLAND, F.S., "The Synergetic Plane Change for Orbiting Spacecraft ", Rand Corporation, Memorandum RM-3231-PR, August 1962.

4. VINH, N.X. and HANSON, J.M., "Optimal Aeroassisted Return form High Earth Orbit with Plane Change," *Acta Astronautica*, Vol. 12, No. 1, 1985, pp. 11-25.

5. DICKMANNS, E.D., "The Effect of Finite Thrust and Heating Constraints on the Synergetic Plane Change Maneuver for a Space Shuttle Orbiter-Class Vehicle," NASA TN D-7211, October 1973.

6. CAUDRA, E. and ARTHUR, P.D., "Orbit Plane Change by External Burning Aerocruise," *Journal of Spacecraft and Rockets*, Vol. 3, March 1966, pp.347-352.

7. CLAUSS, J.S., JR. and YEATMAN, R.D., "Effect of Heating Restraints on Aeroglide Synergetic Maneuver Performance", *Journal of Spacecraft and Rockets*, Vol. 4, August 1967, pp. 1107-1109.

8. PAINE, J.P., "Use of Lifting Re-Entry Vehicles for Synergetic Maneuvers," *Journal of Spacecraft and Rockets*, Vol. 4, No. 5, May 1967, pp. 698-700.

9. BELL, R.N. and HANKEY, W.L., Jr., "Application of Aerodynamic Lift in Accomplishing Orbital Plane Change," ASD-TDR-63-693, September 1963.

10. NYLAND, F.S., "Considerations of Applying Continuous Thrust During Synergetic Plane Changing," Paper 68-121, AAS/AIAA Astrodynamics Specialist Conference, Jackson, Wyoming, Sept. 1968.

11. PARSONS, W.D., "Analytic Solution of the Synergetic Turn," *Journal of Spacecraft*, Vol. 3, No. 11, November 1966, pp. 1675-1678.

12. IKAWA, H. and RUDIGER, T.F., "Synergetic Maneuvering of Winged Spacecraft for Orbital Plane Change," *Journal of Spacecraft and Rockets*, Vol. 19, No. 6, Nov.-Dec. 1982, pp. 13-520.

13. CERVISI, R.T., "Analytic Solution for a Cruising Plane Change Maneuver," *Journal of Spacecraft and Rockets*, Vol. 22, No. 2, Mar.- Apr. 1985, pp. 134-140.

14. BRAUER, G.L., CORNICK, D.E., and STEVENSON, R., "Capabilities and Applications of the Program to Optimize Simulated Trajectories (POST)," NASA CR-2770, Feb. 1977.

15. VINH, N.X., BUSEMANN, A., and CULP, R.D., *Hypersonic and Planetary Entry Flight Mechanics*, University of Michigan Press, Ann Arbor, 1980.

16. HOGE, H.J., "Development of Military Hypersonic Flight Test Experiments." AFFDL-TR-79-3159, AFFDL/FXS Contract F33615-78-C-3020, Nov. 1979.